J Mater Sci (2008) 43:6344–6352
DOI 10.1007/s10853-008-2918-1

Mechanical properties of single- and double-gated injection moulded short glass fibre reinforced PBT/PC composites

A. Khamsehnezhad · S. Hashemi

Received: 10 January 2008 / Accepted: 31 July 2008 / Published online: 16 August 2008

Abstract Tensile and flexural properties of single-gated (SG) and double-gated (DG) injection moulded blend of polybutylene terephthalate (PBT) and polycarbonate (PC) and its composites containing 15, 20 and 30 wt.% short glass fibres were investigated. In the DG mouldings, a weldline was formed by direct impingement of two opposing melt fronts (i.e. cold weld). It was found that tensile modulus was not affected by the weldline but flexural modulus decreased in the presence of weldline. For both specimen types, modulus increased linearly with volume fraction of fibres (ϕ_f), according to the rule-of-mixtures for moduli. The weldline integrity (WIF) factor for flexural modulus decreased linearly with increasing ϕ_f. Results showed that tensile and flexural strengths for SG mouldings increase with increasing ϕ_f in a linear manner according to the "rule-of-mixtures" for strengths. The presence of weldline affected both strengths in a significant way; WIF factor decreased linearly with increasing ϕ_f and was independent of loading mode. It was noted also, that the overall fibre efficiency parameter for tensile modulus was independent of specimen type but for flexural modulus it was lower in the case of DG mouldings. In all cases, efficiency parameter for strength was considerably lower than for the modulus. Impact strength and fracture toughness of SG mouldings were significantly greater than for DG mouldings. Although these properties for SG mouldings increased with increasing ϕ_f, they decreased significantly for DG mouldings. Results showed that WIF factor for impact strength and fracture toughness decreased linearly with increasing ϕ_f.

A. Khamsehnezhad · S. Hashemi (✉)
London Metropolitan Polymer Centre, London Metropolitan University, London, UK
e-mail: s.hashemi@londonmet.ac.uk

Introduction

The mechanical properties of short fibre polymer composites such as strength and modulus are derived from a combination of the fibre and matrix properties and the ability to transfer stresses across the interface between the two constituents. These properties, however, are affected by a number of parameters, most importantly, concentration, length and orientation of the fibres as well as the degree of interfacial adhesion between the fibre and the matrix [e.g. 1–12]. Since most short fibre polymer composites are fabricated using injection moulding process, the presence of weldlines poses a major design concern in multigate mouldings. This is because weldlines could lead to a considerable reduction in mechanical properties hence forcing product designers to incorporate liberal safety factors in design analysis to compensate for this weakness.

Weldlines are classified as either being cold or hot. The cold weldlines are formed when two melt fronts meet head on; this type of weld provides the worst-case scenario as far as mechanical properties are concerned. A serious reduction in strength has been reported for many polymers and their composites in the presence of cold weldlines [e.g. 1–8]. In general, the presence of a weldline reduces the strength by 10–60% depending on the polymer and the characteristic features of the reinforcing filler. However, the integrity of weldlines is mostly assessed in tension and therefore there is limited amount of information on the integrity of weldlines in bending particularly in short fibre composite systems. To this end, the present article was undertaken on single-gated (SG) and double-gated (DG) polybutylene terephthalate (PBT)/polycarbonate (PC) and PBT/PC short glass fibre (GF) composites mainly to compare the integrity of weldlines in both tension and flexure as a function of the fibre concentration ranging from 0 to 30% w/w.

Table 1 Injection moulding processing conditions for PBT/PC and PBT/PC composites

Processing conditions	PBT/PC	Composite with		
		15%w/w fibre	20%w/w fibre	30%w/w fibre
Barrel temperature (°C)				
Zone 1 (nozzle)	280	275	280	280
Zone 2	275	275	280	285
Zone 3	275	275	280	285
Zone 4	275	275	280	285
Mould temperature (°C)	80	80	80	80
Injection pressure (%)	50	50	50	50
Injection speed (%)	85	85	85	85
Cooling time (s)	15	15	15	15

Experimental details

Materials

The matrix material used in this article was a blend of PBT and PC. The blend (PBT/PC) and its composites containing 15, 20 and 30 wt.% short GFs were supplied by Lanxness in the form of pellets for injection mouldling process. The blend and its composites were dried in an air circulating oven for 8 h at 120 °C as recommended by the manufacturer before being injection moulded into test specimens.

Injection moulding

The dried compounds were injection moulded in a Klockner Ferromatik F-60 injection moulding machine at the processing conditions listed in Table 1 to produce dumbbell test specimens. The mould used consisted of an SG and a DG cavities each of nominal dimensions $4 \times 10 \times 120$ mm^3 (thickness, width, length). In the latter, the two opposing melt fronts met to form a weldline approximately a mid-way along the gauge length of the specimen.

Fibre concentration measurements

The exact weight fraction of the fibres in as received compounds (ARC) and in injection moulded specimens (IMS) was determined by ashing a pre-weighed amount of material in a muffle furnace at 550 °C for at least 1 h. After cooling, the remnant was weighed and weight fraction of fibres w_f was determined. It can be seen from Table 2 that the measured weight fractions in ARC and IMS is within 1% of the manufacturer's specification (the scatter associated with each measurement was <2%).

The weight fractions, w_f, were subsequently converted into volume fractions, ϕ_f, using Eq. 1:

Table 2 Fibre concentration and the average fibre lengths in ARC and in IMS

Composites	PBT/PC 15%w/w fibres	PBT/PC 20%w/w fibres	PBT/PC 30%w/w fibres
%w/w (ARC)	15.14	19.99	30.02
%w/w fibre (IMS)	15.64	20.17	30.29
Density (kg/m^3)	1,350	1,400	1,500
%v/v (IMS)	8.31	11.12	17.89
Average fibre length (ARC) (μm)	143 (740)	124 (650)	131 (762)
Average fibre length (IMS) (μm)	115 (650)	118 (774)	126 (718)
Reduction in fibre length (%)	19.6	4.8	3.8

Values given in the parenthesis are the total number of fibre lengths measured

$$\phi_f = \frac{\rho_c}{\rho_f} w_f. \quad (1)$$

Table 2 gives values of ϕ_f obtained using Eq. 1, using GF density, ρ_f, of 2,540 kg m^{-3} and the composite densities values, ρ_c, as provided by the manufacturer.

Fibre length distribution

The ashes of fibrous material were subsequently spread on a glass slide and placed on the observation stage of a microscope. Magnified fibre images were transmitted to a large screen, and the fibre images were then automatically digitised. From the fibre length distributions, examples of which are shown in Fig. 1, the average fibre lengths (L_f) in as ARC and in the moulded specimens (IMS) were determined. The measured values are given in Table 2 where it can be seen that there is not systematic variation in L_f with increasing fibre concentration. It is also evident, that injection moulding process only affected the L_f for composites containing 15% w/w of short fibres, for which the reduction in length of ~20% was incurred. For the other two composites, the change in the average fibre length due to processing was only 3–5%.

Tensile and flexural tests

SG and DG dumbbell specimens were pulled in tension at 25 °C in a Tinius Olsen H10KS testing machine at a crosshead displacement rate of 50 mm/min. From the load–extension curves, tensile strength and modulus values for both specimen types were determined using the initial slope and the load at maximum, respectively.

Flexural tests were performed on rectangular coupons cut from the gauge length of both single and DG dumbbell

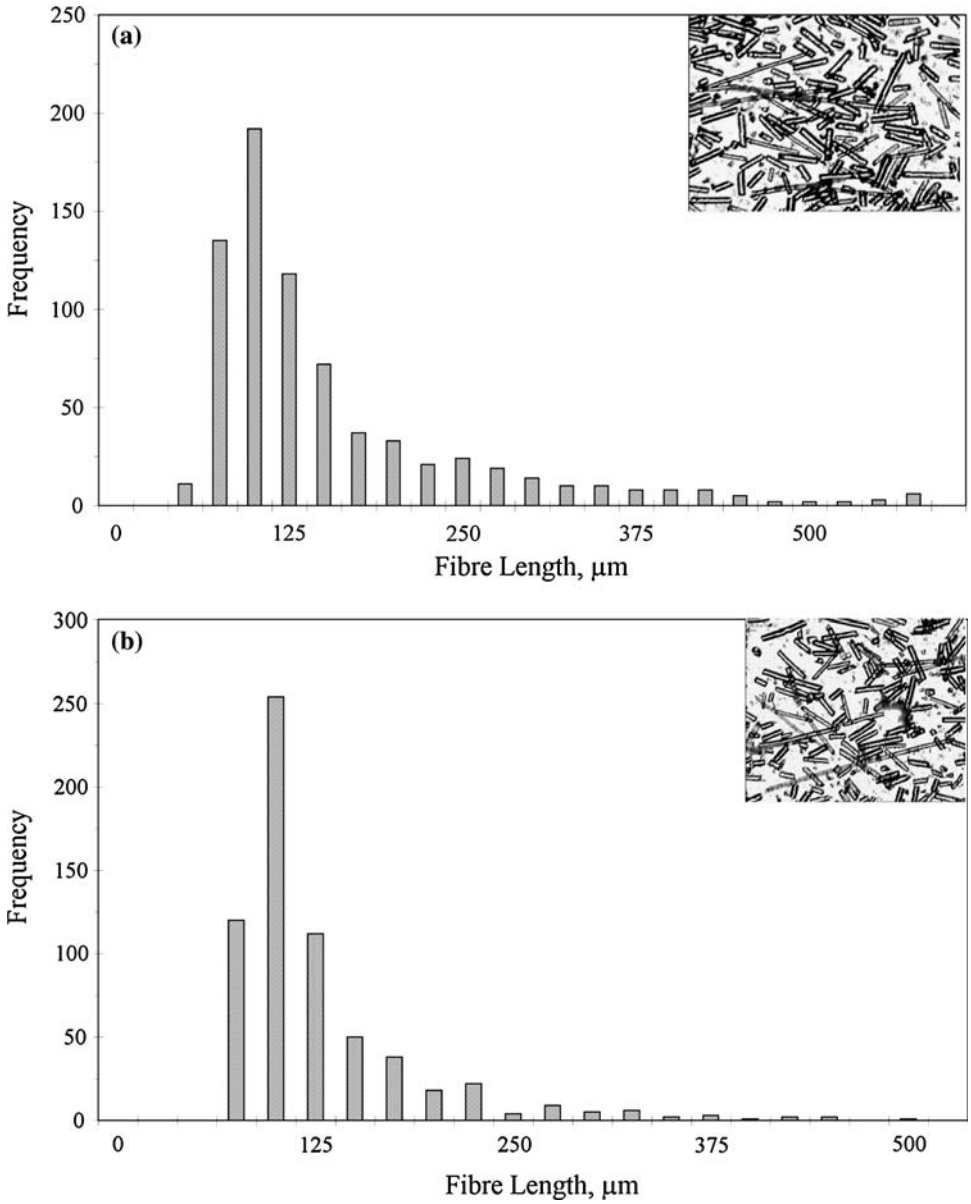

Fig. 1 Fibre length distributions in PBT/PC composite containing 15% w/w short GFs; (**a**) ARC and (**b**) IMS

specimens. Tests were carried out in three-point bend as shown in Fig. 3a over a span width of 64 mm by flexing the coupons flat-wise as shown in Fig. 2a at a crosshead speed of 50 mm/min (strain rate of 4.88×10^{-3}). The DG specimens were positioned on the rig such that weldline was at mid-span, i.e. under the loading nose. The flexural modulus and strength were calculated from the following linear elastic equations:

$$\text{Flexural strength} = \frac{3P_{\max}S}{2BD^2}, \tag{2}$$

$$\text{Flexural modulus} = \frac{k}{4B}\left(\frac{S}{D}\right)^3, \tag{3}$$

where $P_{\max}$ is the load at maximum and k is the specimen given by initial slope of the load–deflection curve.

The effect of weldline on tensile and flexural properties was qualitatively expressed in terms of "weldline integrity (WIF)" defined as;

$$\text{WIF} = \frac{P_w}{P}, \tag{4}$$

where P is the measured property in the absence of weldline and P_w is the same measured property in the presence of weldline. The WIF value of less than unity implies deterioration in the measured property due to weldline.

Fracture toughness (K_C) tests

Fracture toughness tests were performed on rectangular coupons cut from the gauge length of both single and DG

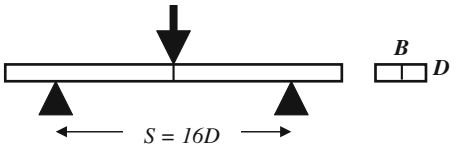

(a) *Flat-wise (B = 10 mm, D = 4 mm)*

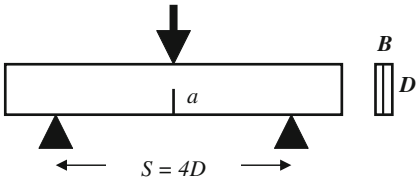

(b) *SENB (B = 10 mm, D = 4 mm)*

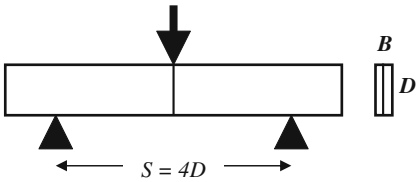

(c) *Edge-wise (B = 4 mm, D = 10 mm)*

Fig. 2 Test specimen geometries

dumbbell specimens. Coupons were notched to various *a/D* ratios (crack length-to-depth ratio) to produce series of single-edge notched bend (SENB) specimens as shown in Fig. 2b. In the case of DG specimens, care was taken to ensure the initial notch was placed inside the weldline region. SENB specimens were subsequently fractured edge-wise in a three-point bend configuration over a span width of 40 mm (i.e. $S/D = 4$) at a crosshead displacement rate of 50 mm/min. The load–deflection curve for each specimen was recorded from which failure load (P_f) was used to calculate fracture toughness, K_{IC} of single and DG specimens using the following equation:

$$K_c = \frac{3P_f S}{2BD^2}\, Y(x)\sqrt{a}, \tag{5}$$

where $x = a/D$. The term $Y(x)$ is the finite width correction factor whose value for $S/D = 4$ was obtained from the following polynomial;

$$Y(x) = 1.93 - 3.07x + 14.53x^2 - 25.11x^3 + 25.80x^4. \tag{6}$$

The weldline effect on fracture toughness was qualitatively expressed in terms of "WIF" defined as;

$$\text{WIF} = \frac{K_C}{K_{Cw}}. \tag{7}$$

In the above equation, K_C is the fracture toughness of the unweld specimen (SG) and K_{Cw} is the fracture toughness of the weld specimen (DG).

Impact strength tests

Charpy impact strength (impact energy per unit area) was determined using rectangular coupons cut from the gauge length of both SG and DG dumbbell specimens. Coupons were impacted edge-wise as in Fig. 2c in a Ray-Ran pendulum impact testing machine at hammer velocity of 2.9 m/s over a span width of 40 mm (i.e. span-to-depth ratio of 4:1).

Weldline effect on impact strength was qualitatively expressed in terms of "WIF" defined as;

$$\text{WIF} = \frac{U}{U_w}, \tag{8}$$

where U is the impact strength of the unweld specimen (SG) and U_w is that of the weld specimen (DG).

Results and discussion

Tensile and flexural modulus

The load–extension and load–deflections curves revealed that the deformation of PBT/PC and its composites during the early stages was linearly elastic for both SG and DG specimens. The stiffness of both specimen types in tension and in flexure increased as concentration of GFs increased.

The effect of fibre concentration on tensile and flexural modulus is shown in Figs. 3 and 4, respectively, for both SG and DG specimens, respectively. As can be seen, elastic modulus for both specimen types increases linearly with increasing ϕ_f. However, whilst tensile modulus is not affected by the presence of weldline (DG specimens), flexural modulus is reduced. Indeed, as illustrated in Fig. 5, weldline integrity factor for tensile modulus is near unity, whereas for flexural modulus it decreases almost linearly

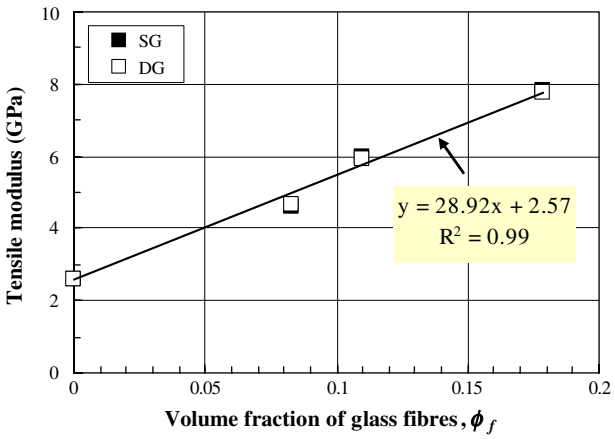

Fig. 3 Tensile modulus versus volume fraction of GFs for SG and DG specimens

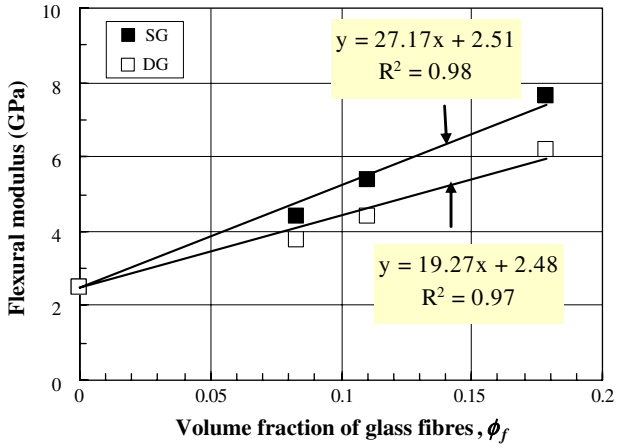

Fig. 4 Flexural modulus versus volume fraction of GFs for SG and DG specimens

with increasing ϕ_f. In flexure tests, the loading nose was rested on the weldline region hence stiffness of the specimens in flexure was more affected by the weakness of the weldline than in tension where the load was applied remote for the weldline and therefore the early stages of the deformation was not influenced by the presence of the weldlines.

Using the linear regression parameters shown in Fig. 5 results in the following relationship between weld and unweld flexural modulus and volume fraction of GFs;

$$E_{cw} = E_c\,(1 - 1.13\phi_f), \tag{9}$$

where E_{cw} and E_c are weld and unweld flexural modulus, respectively.

The linear dependence between composite modulus and volume fraction of fibres for both SG (unweld) and DG (weld) specimens in tension and in flexure indicated that the data in Figs. 3 and 4 can be modelled using a simple rearrangement of the "rule-of-mixtures" equation:

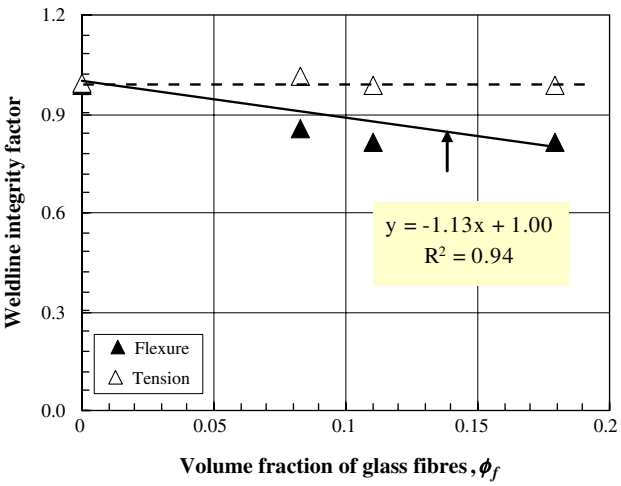

Fig. 5 WIF for tensile and flexural modulus versus volume fraction of GFs

$$E_c = E_m + (\eta_E E_f - E_m)\phi_f, \tag{10}$$

where E_m is the modulus of the matrix and E_f is the modulus of the fibre whose value in this article was taken as 76 GPa. The parameter η_E is termed the "overall fibre efficiency" for the composite modulus. The efficiency parameter η_E whose value depends on the length and the orientation of the fibres in the moulded specimens can be obtained from the slope of the regression lines shown in Figs. 3 and 4. Linear regression values of η_E for both SG and DG specimens are given in Table 3. Note that whilst in tension η_E is independent of the specimen type, in flexure η_E is dependent upon the specimen type having a greater value for SG specimens than for DG counterparts. It is worth noting also, that the value of η_E for SG mouldings is not significantly affected by the mode of loading.

The overall efficiency parameter η_E is the product of two efficiency parameters as stated by Eq. 11; one associated with the orientation of the fibres (η_o) and the other with the shortness of the fibres (η_L).

$$\eta_E = \eta_L \eta_o. \tag{11}$$

The parameter η_L may be evaluated using the Cox shear lag model [13] which gives the following expressions for η_L:

$$\eta_L = 1 - \frac{\tanh\beta}{\beta}, \tag{12}$$

where β is defined as;

$$\beta = \frac{L_f}{2}\left(\frac{4E_m}{E_f d^2 \ln\lambda}\right)^{\frac{1}{2}}, \tag{13}$$

where d is the diameter of the fibres. If packing arrangement of fibres is assumed square, then λ can be obtained from the following relationship;

Table 3 Fibre efficiency parameters for tensile and flexural modulus

ϕ_f	L_f	η_E	η_L	η_o	$\theta°$
SG and DG mouldings in tension					
0.083	115	0.414	0.455	0.910	12.39
0.111	118	0.414	0.494	0.838	16.91
0.179	126	0.414	0.578	0.717	23.05
SG mouldings in flexure					
0.083	115	0.391	0.449	0.871	14.97
0.111	118	0.391	0.488	0.801	18.91
0.179	126	0.391	0.572	0.683	24.62
DG mouldings in flexure					
0.083	115	0.289	0.447	0.627	27.15
0.111	118	0.289	0.486	0.577	29.36
0.179	126	0.289	0.570	0.491	33.17

$$\lambda = \sqrt{\frac{\pi}{4\phi_f}}. \tag{14}$$

Values of η_L obtained using Eqs. 12 and 13 for both SG and DG specimens in tension and flexure are presented in Table 3 together with the corresponding η_o values obtained from the ratio η_E/η_L. As can be seen, fibre efficiency parameters η_L and η_o for both SG and DG specimens are functions of the fibre concentration with reduced values at higher fibre concentration. The decrease in η_o with increasing ϕ_f indicates a mutual influence of the fibres hindering the orientation formation. Using the Krenchel [14] definition of η_o which is given by Eq. 15 (assuming a perfect alignment of fibres), one can determine the average fibre orientation angle, θ with respect to the loading direction.

$$\theta = \mathrm{Cos}^{-1}\,[\eta_o]^{\frac{1}{4}}. \tag{15}$$

The values of θ calculated using Eq. 15 are also presented in Table 3, where it can be seen that θ is more or less independent of loading mode but increases with increasing ϕ_f. It is also evident that in flexure, values of θ for DG specimens are about 10° greater than for SG counterpart.

Tensile and flexural strength

The deformation curves (load–extension and load–deflection curves) for both SG and DG specimens revealed that failure of the specimens was essentially brittle. However, in the case of matrix, failure of SG specimens occurred after some degree of plastic deformation. It was noted that the presence of weldlines in DG specimens considerably reduced the amount extension and deflection at break. Further more, whilst matrix failure load was not affected by the specimen type, failure load of DG composites was significantly lower than their SG counterparts, in both tension and flexure. The close examination of the DG specimens indicated that composite specimens failed at the weldline region, whereas matrix specimens failed outside the weldline region. This observation implies that weldline was not the weakest part of the DG matrix specimens.

The effect of fibre concentration on tensile and flexural strengths of SG and DG specimens is shown in Figs. 6 and 7. It can be seen that whilst in both data sets, the specimen type had no significant influence upon the strength properties of the matrix material ($\phi_f = 0$), it had a significant influence upon strength properties of its composites. Clearly, SG composites have much greater tensile and flexural strengths than their DG counterparts and whilst strength values of SG composites increased linearly with increasing ϕ_f, they decreased in the case of DG composites.

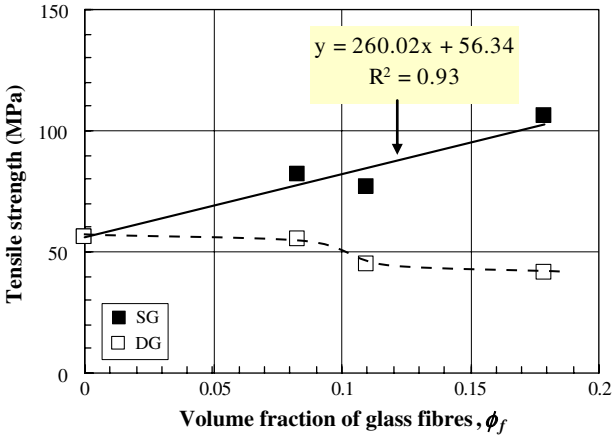

Fig. 6 Tensile strength of SG and DG specimens versus volume fraction of GFs

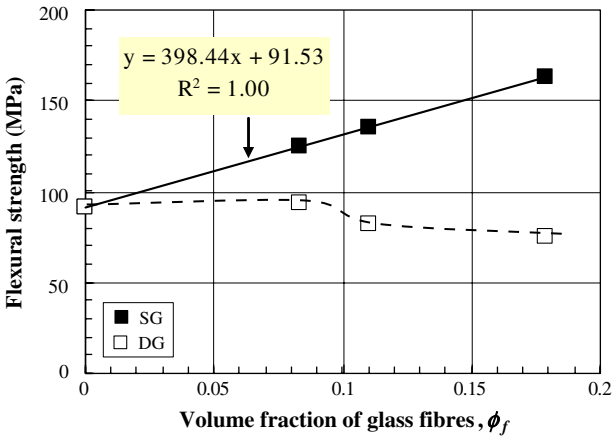

Fig. 7 Flexural strength of SG and DG specimens versus volume fraction of GFs

Results therefore indicate that the extent, to which tensile and flexural strengths of DG specimens are deteriorated due to the presence of weldlines, is dependent upon the concentration of the GFs in the composite.

The effect of weldlines on tensile and flexural strengths is quantitatively expressed in Fig. 8 in terms of WIF. It is interesting to note that WIF is not significantly affected by the loading type and decreases linearly with increasing ϕ_f. The linear regression parameters shown in Fig. 8 result in the following relationship between weld and unweld composite strengths and the volume fraction of GFs;

$$\sigma_{cw} = \sigma_c\,(1 - 3.38\,\phi_f), \tag{16}$$

where σ_{cw} and σ_c are weld (DG) and unweld (SG) composite strengths, respectively.

The linearity of tensile and flexural strengths of SG specimens with volume fraction of fibres implies that like data for modulus the strength data in Figs. 6 and 7 can be modelled using a simple rearrangement of rule-of-mixtures:

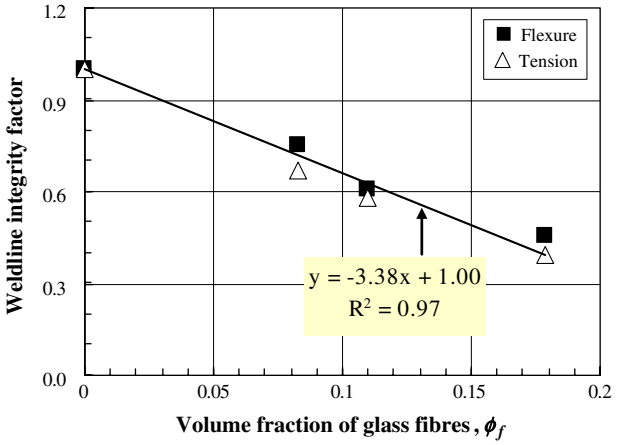

Fig. 8 WIF for tensile and flexural strengths versus volume fraction of GFs

$$\sigma_c = \sigma_m + (\eta_\sigma \sigma_f - \sigma_m)\phi_f, \tag{17}$$

where σ_f and σ_m are strengths of the fibre and the matrix, respectively. The parameter η_σ is termed the overall fibre efficiency for composite strength taking into account the effects due to fibre length and fibre orientation in the composite. Using the slope of the regression lines as shown in Figs. 6 and 7 and tensile and flexural strengths of the GF as 2,470 MPa and 3,705 MPa, respectively, one obtains $\eta_\sigma \approx 0.128$ for tensile strength and $\eta_\sigma \approx 0.132$ for flexural strength (note that flexural strength for GF is calculated using the tensile strength and the Weibull modulus of 5 for glass [15]). It is interesting to note that η_σ is considerably smaller than η_E. Its meaning that composite strength is more affected by the shortness and misalignment of the fibres than the modulus.

The overall efficiency parameter η_σ like η_E is the product of two efficiency parameters as defined by Eq. 18:

$$\eta_\sigma = \eta_L \eta_o. \tag{18}$$

In the above equation, η_L and η_o are the fibre length and orientation efficiency parameters for composite strength, respectively. Using the η_o values obtained via the modulus data (see Table 3), η_L for tensile and flexural strengths was determined from Eq. 18. It can be seen from the values given in Table 4 that η_L for composite strength like the composite modulus decreases with increasing ϕ_f.

Table 4 Fibre efficiency parameters for tensile and flexural strengths

ϕ_f	L_f	Tensile strength		Flexural strength	
		η_σ	η_L	η_σ	η_L
0.083	115	0.128	0.131 *(0.141)*	0.132	0.131 *(0.152)*
0.111	118	0.128	0.135 *(0.153)*	0.132	0.135 *(0.165)*
0.179	126	0.128	0.144 *(0.179)*	0.132	0.144 *(0.193)*

It is well known that the strength of short fibre composites depends largely on the ratio L_c/L_f where L_f is the average length and L_c is the critical length of the fibre, respectively. The value of L_c can be obtained from the following relationship:

$$L_c = \frac{d\sigma_f}{2\tau_m}, \tag{19}$$

where d is the diameter of the fibre (=10 μm), σ_f is tensile strength of fibre and τ_m is shear strength of the matrix whose value in this study is assumed to be half the tensile strength value (i.e. 28.17 MPa). Using Eq. 18 one obtains $L_c \approx 438$ μm, meaning that the measured fibre length averages are less than the critical value. According to Kelly–Tyson [16], when $L_f < L_c$, the efficiency parameter, η_L, is given by:

$$\eta_L = \frac{L_f}{2L_c}. \tag{20}$$

Values of η_L calculated using Eq. 20 are given in the parenthesis in Table 4. It is interesting to note that η_L for composite strength is smaller than that for composite modulus and likewise increases with increasing ϕ_f. This shows that composite strength is more affected by the shortness of the fibres than composite modulus. In addition, the η_L values were also calculated using Eq. 18 and these are given in parenthesis in Table 4. It can be seen that the agreement between the two sets of values is reasonable.

Fracture toughness

In all cases, initial crack propagated normal to the direction of the applied load. The failure load of DG specimens was always lower than that of the SG counterpart. All SG and DG specimens exhibited brittle, linear elastic behaviour with almost all of the energy being used in crack initiation rather than propagation. The K_C values for both specimen types as obtained using the failure load and Eq. 5 are shown in Fig. 9 as plots of K_C versus *a/D*. Plots show that K_C for both specimen types is independent of *a/D*, thus verifying the applicability of the linear elastic fracture mechanics. Its also evident that K_C for DG specimens is significantly lower than SG counterparts, merely reflecting the trend observed in their respective strength values. This observation implies that the material inside the weldline region offers less resistance to crack propagation than the bulk material. This is due to the alignment of the fibres in the weldline region being predominantly parallel to the weldline hence in line with crack propagation direction as opposed to being predominantly normal to crack propagation direction in the bulk material which is the case for SG mouldings.

Figure 10 shows that whilst K_C of the SG specimens increases with fibre concentration, that of the DG specimens rises initially before decreasing with increasing fibre

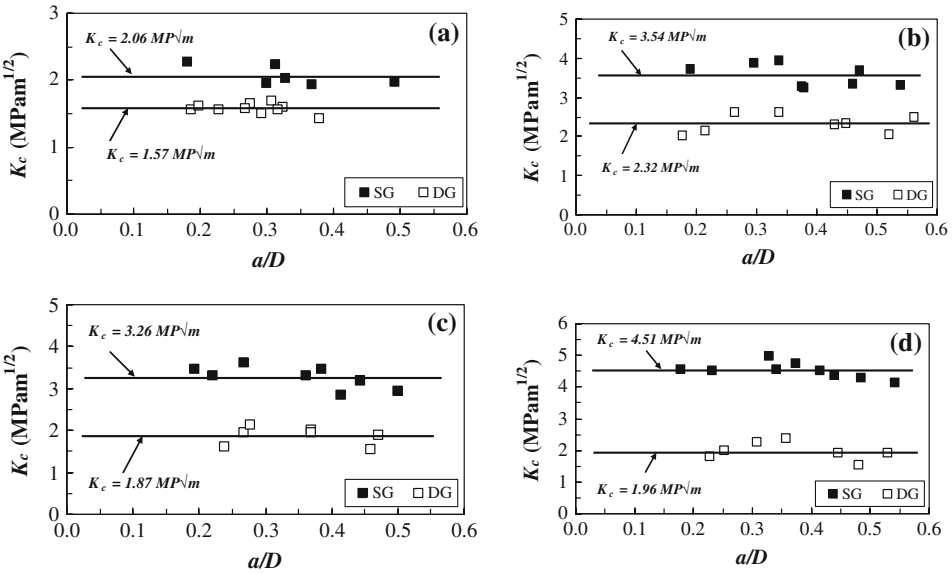

Fig. 9 Fracture toughness versus *a/D* for single and DG specimens. (**a**) 0% GF, (**b**) 15% GF, (**c**) 20% GF, (**d**) 30% GF

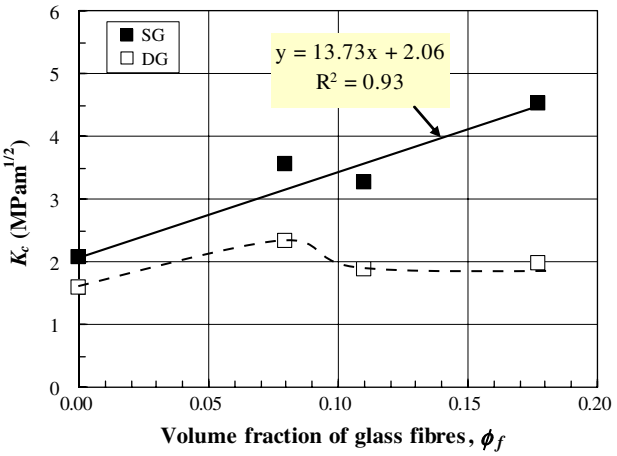

Fig. 10 Fracture toughness, K_c, of SG and DG specimens versus volume fraction of GFs, ϕ_f

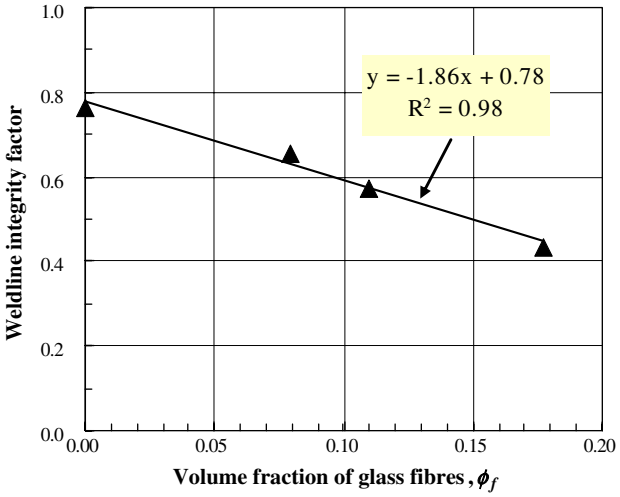

Fig. 11 WIF for fracture toughness versus volume fraction of GFs

concentration. It is worth noting that the variation of K_C with fibre concentration for both SG and DG mouldings is similar to that of flexural strength (or tensile strength) versus fibre concentration, for the two specimen types as shown in Fig. 9.

The effect of weldline on fracture toughness is quantitatively expressed in terms of WIF as defined by Eq. 7. As shown in Fig. 11, WIF decreases linearly with increasing ϕ_f. Using the regression line shown in Fig. 11, one obtains the following relationship between weld and unweld fracture toughness values and the volume fraction of fibres

$$K_{Ccw} = K_{Cc}(0.78 - 1.86\phi_f), \quad (21)$$

where K_{Cc} is the fracture toughness of the unweld composite and K_{Ccw} is the corresponding value of the weld counterpart.

According to Fig. 10, fracture toughness of SG specimens increases linearly with increasing ϕ_f. The linear regression line in Fig. 10 gives the following relationship:

$$K_{Cc} = K_{Cm}(1 + 6.67\phi_f), \quad (22)$$

where K_{Cc} is the fracture toughness of the unweld composite and K_{Cm} is the corresponding value for the matrix.

Impact strength

The impact strength of SG and DG specimens is compared in Fig. 12 as a function of fibre concentration. It is evident that impact strength of SG specimens is always greater than impact strength of the DG specimens, and whilst the value for SG mouldings increases with increasing fibre concentration, it decreases in the case of DG mouldings. This observation implies that weldlines could seriously affect impact performance of the DG mouldings.

The effect of weldline on impact strength is quantitatively expressed in terms of WIF as defined by Eq. 8. It can

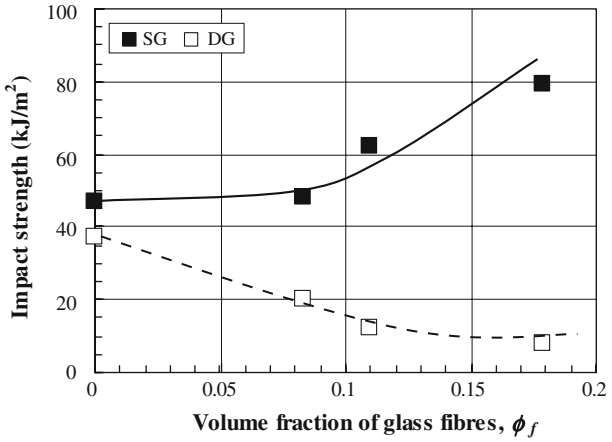

Fig. 12 Impact strength of SG and DG specimens versus volume fraction of GFs

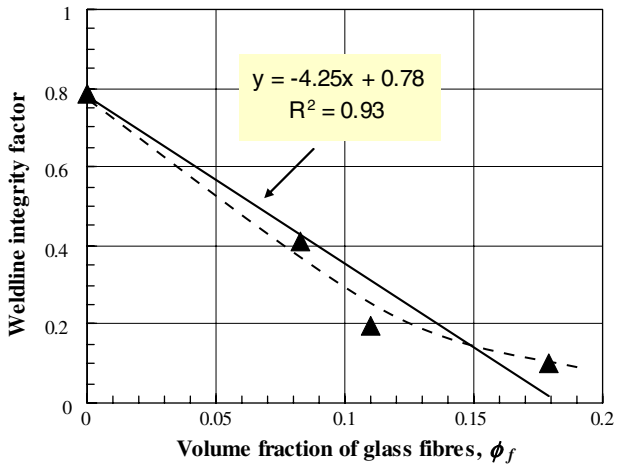

Fig. 13 WIF for impact strength versus volume fraction of GFs

be seen from Fig. 13 that WIF for impact strength decreases significantly with increasing ϕ_f and can be assumed to be reasonably linear. The regression line in Fig. 13 gives the following relationship between weld and unweld impact strengths.

$$U_{cw} = U_c(0.78 - 4.25\phi_f). \quad (23)$$

In the above equation U_c is the unweld impact strength for the composite and U_{cw} is the corresponding value for the weld.

Conclusions

Mechanical and fracture properties of SG and DG PBT/PC and PBT/PC composites containing 10, 20 and 30 wt.% short GFs were studied. The following observations were made:

- Tensile and flexural modulus of SG and DG specimens increased linearly with increasing ϕ_f according to the modified "rule-of-mixtures" for short fibre composites. It was noted that whilst tensile modulus of the DG composites was not affected by the weldline, flexural modulus dropped by as much as 20% for composite containing 30 wt.% short fibres.
- Tensile and flexural strengths of SG mouldings increased linearly with increasing ϕ_f according to the modified "rule-of-mixtures" for short fibre composites. On the other hand, strength values of DG mouldings decreased nonlinearly with increasing ϕ_f. WIF for composite strength decreased almost linearly with increasing ϕ_f, showing no loading mode effect.
- The overall fibre efficiency parameter for composite strength, η_σ, was always greater than for composite modulus, η_E. Although η_E for tensile modulus was not affected by the weldline, η_E for flexural modulus was dropped in the presence of weldlines. η_σ, for tensile and flexural strengths were reduced in the presence of weldlines.
- Impact strength and fracture toughness of the SG mouldings increased, but for DG mouldings it decreased, with increasing ϕ_f. Weldline integrity parameter for both properties decreased almost linearly with increasing ϕ_f.

References

1. Hashemi S, Gilbride MT, Hodgkinson JM (1996) J Mater Sci 31:5017. doi:10.1007/BF00355900
2. Din KJ, Hashemi S (1997) J Mater Sci 32:375. doi:10.1023/A:1018553400266
3. Chrysostomou A, Hashemi S (1998) J Mater Sci 33:1165. doi:10.1023/A:1004365323620
4. Chrysostomou A, Hashemi S (1998) J Mater Sci 33:4491. doi:10.1023/A:1004487814709
5. Nabi ZU, Hashemi S (1998) J Mater Sci 33:2985. doi:10.1023/A:1004362915713
6. Hashemi S (2002) J Plast Rubber Compos 31:1. doi:10.1179/146580101125000484
7. Hashemi S, Lepessova Y (2007) J Mater Sci 42:2652. doi:10.1007/s10853-006-1358-z
8. Necar M, Irfan-ul-Haq M, Khan Z (2003) J Mater Process Technol 142:247. doi:10.1016/S0924-0136(03)00567-3
9. Fu SY, Lauke B, Mader E, Yue CY, Hu X (2000) Composites A 31:1117
10. Fisa B (1985) Polym Compos 6:232. doi:10.1002/pc.750060408
11. Thomason JL (2002) Compos Sci Technol 62:1455. doi:10.1016/S0266-3538(02)00097-0
12. Thomason JL (2001) Compos Sci Technol 61:2007. doi:10.1016/S0266-3538(01)00062-8
13. Cox HL (1952) Br J Appl Phys 3:72. doi:10.1088/0508-3443/3/3/302
14. Krenchel H (1964) Fibre reinforcement. Akademisk Forlag, Copenhagen
15. Courtney TH (1990) Mechanical behaviour of materials. McGraw-Hill International Editions
16. Kelly A, Tyson WR (1965) J Mech Phys Solids 13:329. doi:10.1016/0022-5096(65)90035-9